

Anti-windup compensator design for power system subjected to time-delay and actuator saturation

eISSN 2515-2947
 Received on 9th July 2018
 Revised 10th October 2018
 Accepted on 21st November 2018
 E-First on 23rd January 2019
 doi: 10.1049/iet-stg.2018.0113
 www.ietdl.org

Maddela Chinna Obaiah¹ ✉, Bidyadhar Subudhi¹

¹Department of Electrical Engineering, National Institute of Technology, Rourkela, India

✉ E-mail: chinnaobaiah.m@gmail.com

Abstract: In this study, a delay-dependent anti-windup compensator (AWC) is designed for supplementary damping control (SDC) of flexible AC transmission system (FACTS) device to enhance the damping of inter-area oscillations of the power system subjected to time-delay and actuator saturation. By employing global signal measurements, an SDC of FACTS device is designed without considering the effect of time-delay and actuator saturation to stabilise the power system using a robust output feedback controller with pole placement approach. Then, based on the generalised sector condition and Lyapunov–Krasovskii functional, an add-on delay-dependent AWC is designed to mitigate the adverse effect of time-delay and actuator saturation non-linearity. For the design of delay-dependent AWC, sufficient conditions guarantee the asymptotic stability of the closed-loop power system are formulated in the form of linear matrix inequalities (LMIs). These conditions are cast into the LMI-based convex optimisation problem to compute the AWC gains. To evaluate the effectiveness of the proposed controller, non-linear simulations were performed first using MATLAB/Simulink. Then, the authors implemented the proposed controller in real-time using the Opal-RT digital simulator. From the obtained results, it is observed that the proposed controller enhances the damping of inter-area oscillations by compensating the effect of time delay and actuator saturation.

1 Introduction

Inter-area oscillations with frequency range 0.2–0.8 Hz are one of the main concerns of the power system operators which are resulted when the two or more coherency groups of generators swing against each other [1]. The poor damping of these oscillations reduces the power transfer capacity of the transmission lines between the areas and even causes the system instability. Power system stabilisers (PSSs) [2–4] and flexible AC transmission system (FACTS) [5–7] with supplementary damping control (SDC) based on wide-area measurement systems provide sufficient damping to the inter-area oscillations by using remote feedback signals [8]. These signals from phasor measurement units to the control centre and control centre to actuators are transferred through a packet-based communication network. The usage of a communication network in the feedback loop introduces new problems such as time-delays which deteriorate the control performance or may even cause the closed-loop system instability [9]. The duration of time delays depends on the transferred distance, type of the communication network and protocol used for transmission. Therefore, it is important to consider the time delays in the process of damping controller design and find the time delay margin under which wide-area power system remains stable. Various damping controller design techniques are reported in the literature to guarantee the stability of the system by compensating the effect of time-delays [2, 4, 6, 10–12]. In [13–16], the damping controllers are proposed to compensate the time-delays that occur in the feedback loop based on model predictive control strategy.

On the other hand, actuator saturation is an inevitable nonlinear phenomenon in a control system due to the physical limitations or safety reasons; the actuator output signal is limited by its minimum and maximum values. The presence of actuator saturation leads to degradation of performance of the closed-loop system or even makes it unstable [17–19]. Several approaches have been proposed in the literature to address the stability of the system under actuator saturation [20–22], e.g. direct approach and indirect approach. In the direct approach, the actuator saturation is considered at the beginning of control design process [20], while in the indirect approach, a conventional controller designed first without considering saturation and then an add-on anti-windup

compensator (AWC) is designed to minimise the adverse effect caused by the actuator saturation non-linearity [21, 22]. Among these two approaches, an indirect approach which is also known as an anti-windup method is the most popular in practice.

Most of the power system controllers usually have saturation limits which are resulted from the safety reason or physical limitation of the equipment rating. These saturation limits restrict the output signal of the damping controller within the range of permissible values which in turn reduce the signal need for the damping of inter-area oscillations and therefore affect the overall closed-loop system performance [23]. In power system literature, very limited research has been directed on the effect of actuator saturation on the power system stability [24–27]. However, these works have not considered the effect of time-delays. If the actuator saturation and time-delays are not properly accounted in the damping controller design, they deteriorate the overall performance of the system and even lead to the system instability.

Motivated by this, in this paper, to compensate the effect of time-delays and actuator saturation, an AWC is designed by using a delay-dependent Lyapunov–Krasovskii functional and generalised sector conditions for the SDC of the FACTS devices. The H_∞ output feedback controller with a pole-placement approach reported in [28] is considered for the design of SDC. The performance of the proposed controller has been verified in both MATLAB/Simulink and real-time experimentation pursued on OPAL-RT, a real-time digital simulator. The structure of the proposed controller with the power system is shown in Fig. 1. Throughout the paper, the design of an AWC with H_∞ output feedback control with pole placement is referred to as our proposed controller. The contributions of the paper are as follows:

- This paper deals with the effect of both time-delay and actuator saturation on the damping of inter-area oscillations of the power system.
- To compensate for the effect of both time-delay and actuator saturation, we propose a delay-dependent AWC for SDC of FACTS devices.
- Sufficient conditions for the asymptotic stability of the system are formulated in the form of linear matrix inequalities (LMIs)

based on Lyapunov–Krasovskii functional and generalised sector conditions.

- To compute the AWC gains, these conditions are cast into the following convex optimisation problem: the minimisation of the L_2 gain of the disturbance to the system regulated output.
- The effectiveness of the proposed controller is validated on a two-area four-machine power system with a thyristor controlled series capacitor (TCSC) in both MATLAB/Simulink and OPAL-RT real-time digital simulator.

The remaining of the paper is organised as follows. The problem formulation and some related preliminaries are presented in Section 2. In Section 3, an anti-windup synthesis with time-delay is presented by using Lyapunov–Krasovskii functional. In Section 4, a two-area four-machine power system is considered as a case study to validate the effectiveness of the proposed controller and presented simulation results. In Section 5, experimental results by using Opal-RT real-time simulator are presented. Section 6 provides the conclusions.

Notation: Throughout this paper, \mathfrak{R}^n denotes the n -dimensional Euclidean space. $\mathfrak{R}^{n \times m}$ is the set of all $n \times m$ real matrices. The superscripts $'$ and -1 define transpose and the inverse of a matrix, respectively. $P = P' > 0$ (≥ 0) denotes that P is a real symmetric positive-definite (positive semi-definite) matrix. $\text{diag}\{\dots\}$ denotes a block-diagonal matrix. I denotes the identity matrix with appropriate dimensions. The symmetric term in a symmetric matrix is denoted by $*$.

2 Problem formulation and preliminaries

An inter-connected power system consists of various components such as synchronous generators with their excitation systems (IEEE-ST1A), PSSs, and FACTS controllers such as TCSC, SVC, and several loads. The above components are inter-connected through a transmission network. An inter-connected power system with components above is represented by a set of non-linear differential and algebraic equations (DAEs) are presented in [29].

The linearised state-space form of the pre-fault open-loop power system by excluding the damping controller at an equilibrium point is given by

$$\left. \begin{aligned} \dot{x}(t) &= Ax(t) + B_\omega \omega(t) + Bu(t) \\ y(t) &= C_y x(t) \\ z(t) &= C_z x(t) + D_z u(t) \end{aligned} \right\} \quad (1)$$

where $x(t) \in \mathfrak{R}^n$, $u(t) \in \mathfrak{R}^m$, $y(t) \in \mathfrak{R}^p$, $z(t) \in \mathfrak{R}^{n_z}$ and $\omega(t) \in \mathfrak{R}^{n_\omega}$ are the vectors of state variables, control inputs, measured outputs, regulated outputs and exogenous inputs, respectively. A , B , C_y , C_z and D_z are constant real matrices with appropriate dimension.

$\omega(t) \in \mathfrak{R}^{n_\omega}$ is exogenous input which consists of different disturbances, bounded by some scalar δ with limited energy, i.e. $\omega(t) \in L_2$ and it is represented as follows:

$$\|\omega(t)\|_2^2 = \int_0^\infty \omega'(t)\omega(t) dt \leq \frac{1}{\delta}, \quad 0 \leq \frac{1}{\delta} < \infty. \quad (2)$$

In low-frequency inter-area oscillation studies, the fast dynamics are not considered. Hence, the full-order model of the system is not necessary to consider in controller design. To simplify and speed up the controller design procedure, it is necessary to reduce the system order. By employing *Schur* model reduction method [30], the full-order model is reduced where only the poorly damped electromechanical modes are obtained. The linearised reduced model (1) can be written as

$$\left. \begin{aligned} \dot{x}_p(t) &= A_p x_p(t) + B_\omega \omega(t) + B_p u(t) \\ y(t) &= C_1 x_p(t) \\ z(t) &= C_2 x_p(t) + D_2 u(t) \end{aligned} \right\} \quad (3)$$

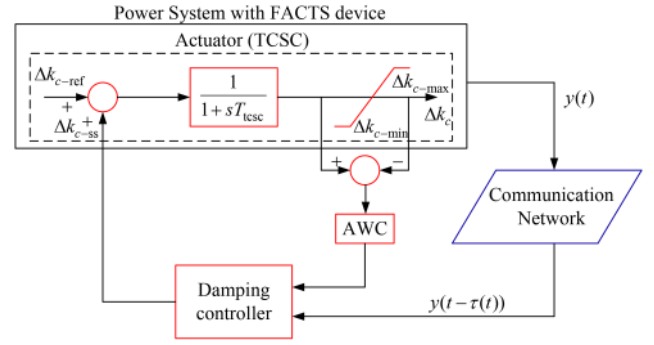


Fig. 1 Block diagram of power system with an anti-windup control

where $x_p(t) \in \mathfrak{R}^{n_p}$ is the vector of reduced-order state variables and A_p , B_p , C_1 , C_2 and D_2 are known constant reduced real matrices with appropriate dimensions.

To enhance the damping of inter-area oscillations of power system described by (3), we consider the following dynamic output feedback controller in the absence of time delays and actuator saturation:

$$\begin{aligned} \dot{x}_c(t) &= A_c x_c(t) + B_c y(t) \\ y_c(t) &= C_c x_c(t) \end{aligned} \quad (4)$$

where $x_c \in \mathfrak{R}^{n_c}$, $y \in \mathfrak{R}^p$ and $y_c \in \mathfrak{R}^m$ are the vectors of controller states variable, controller input and controller output, respectively.

In this paper, H_∞ mixed-sensitivity formulation with robust pole placement approach presented in [28] is considered to design controller (4) to enhance the damping of inter-area oscillation in the absence of time delays and actuator saturation.

Remark 1: For system (3), if there exist $n_p \times n_p$ matrices $R > 0$, $S > 0$, $n_c \times n_c$ matrix \hat{A} , $n_c \times p$ matrix \hat{B} and $m \times n_c$ matrix \hat{C} such that, [28]

$$\begin{bmatrix} R & I \\ * & S \end{bmatrix} > 0 \quad (5)$$

$$\begin{bmatrix} \lambda_{ij} [R & I \\ * & S] + \mu_{ij} \Phi + \mu_{ji} \Phi' \end{bmatrix}_{i,j} < 0 \quad (6)$$

$$\begin{bmatrix} \Lambda_{11} & \Lambda'_{21} \\ * & \Lambda_{22} \end{bmatrix} < 0 \quad (7)$$

where

$$\Phi = \begin{bmatrix} A_p R + B_p \hat{C} & A_p \\ \hat{A} & S A_p + \hat{B} C_1 \end{bmatrix}$$

$$\Lambda_{11} = \begin{bmatrix} A_p R + R A'_p + B_p \hat{C} + \hat{C}' B'_p & B_\omega \\ * & -\gamma I \end{bmatrix}$$

$$\Lambda_{21} = \begin{bmatrix} \hat{A} + A'_p & S B_\omega \\ C_2 R + D_2 \hat{C} & 0 \end{bmatrix}$$

$$\Lambda_{22} = \begin{bmatrix} A'_p S + S A_p + \hat{B} C_1 + C'_1 \hat{B}' & C'_2 \\ * & -\gamma I \end{bmatrix}$$

Moreover, matrices M and N are formulated from singular value decomposition (SVD) of $I - RS$, namely

$$M N' = I - RS. \quad (8)$$

Then the parameter of the dynamic output feedback controller in the form of (4) that places the closed-loop poles in the region \mathfrak{D} can be computed as

$$\begin{aligned} C_c &= \hat{C}(M')^{-1} \\ B_c &= N^{-1}\hat{B} \end{aligned} \quad (9)$$

$$A_c = N^{-1}(\hat{A} - N\hat{B}C_1R - SB_p\hat{C}M' - SA_pR)(M')^{-1}.$$

Consider a time-varying delay in the feedback loop in Fig. 1. To avoid the effect of time-varying delay, the controller (4) can be rewritten as follows:

$$\begin{aligned} \dot{x}_c(t) &= A_c x_c(t) + B_c y(t - \tau(t)) \\ y_c(t) &= C_c x_c(t) \end{aligned} \quad (10)$$

where $\tau(t)$ denotes the time-varying delay that occurs in the feedback loop. The time-varying delay $\tau(t)$ is a continuous differentiable function assumed to be unknown and satisfies the following condition:

$$0 \leq \tau(t) \leq h, \quad \dot{\tau}(t) \leq d \leq 1, \quad (11)$$

where h and d denote upper bound of the time-delay and its rate, respectively.

Consider that the controller output is saturated by following limits:

$$\text{sat}(y_c(t)) = \begin{cases} y_{c_{\max}} & \text{if } y_c \geq y_{c_{\max}} \\ y_c & \text{if } y_{c_{\min}} < y_c < y_{c_{\max}} \\ y_{c_{\min}} & \text{if } y_c \leq y_{c_{\min}} \end{cases} \quad (12)$$

In the presence of actuator saturation, the open-loop system (3) can be expressed as

$$\begin{aligned} \dot{x}_p(t) &= A_p x_p(t) + B_\omega \omega(t) + B_p \text{sat}(y_c(t)) \\ y(t) &= C_1 x_p(t) \\ z(t) &= C_2 x_p(t) + D_2 \text{sat}(y_c(t)) \end{aligned} \quad (13)$$

where $u(t) = \text{sat}(y_c(t))$

The designed damping controller (4) guarantees the stability of the closed-loop system in the absence of time-delay and actuator saturation. To mitigate the effect of time-delays and actuator saturation simultaneously, the controller is modified by adding an AWC using a dead-zone sector non-linearity as follows:

$$\begin{aligned} \dot{x}_c(t) &= A_c x_c(t) + B_c y(t - \tau(t)) + E_c (y_c(t) - \text{sat}(y_c(t))) \\ y_c(t) &= C_c x_c(t) \end{aligned} \quad (14)$$

where E_c is a static AWC gain, the effect of AWC's takes place only when the saturation occurs.

To mitigate the effects of time-delays and actuator saturation, from (11) and (12), the closed-loop power system becomes

$$\begin{aligned} \dot{x}_p(t) &= A_p x_p(t) + B_\omega \omega(t) + B_p \text{sat}(C_c x_c(t)) \\ \dot{x}_c(t) &= A_c x_c(t) + B_c C_1 x_p(t - \tau(t)) + E_c (C_c x_c(t) - \text{sat}(C_c x_c(t))) \\ z(t) &= C_2 x_p(t) + D_2 \text{sat}(C_c x_c(t)) \\ y_c(t) &= C_c x_c(t) \end{aligned} \quad (15)$$

Define an augmented vector as

$$\eta(t) = \begin{bmatrix} x_p \\ x_c \end{bmatrix} \in \mathfrak{R}^{n_p \times n_c} \quad (16)$$

and the matrices are given by

$$\begin{aligned} A_{cl} &= \begin{bmatrix} A_p & B_p C_c \\ 0 & A_c \end{bmatrix}, \quad A_d = \begin{bmatrix} 0 & 0 \\ B_c C_1 & 0 \end{bmatrix}, \quad B_{cl} = \begin{bmatrix} B_p \\ 0 \end{bmatrix}, \\ \mathbb{R} &= \begin{bmatrix} 0 \\ I_{n_c} \end{bmatrix}, \quad B_{cl,\omega} = \begin{bmatrix} B_\omega \\ 0 \end{bmatrix}, \quad C_{cl,z} = [C_2 \quad D_2 C_c], \\ D_{cl,z} &= [D_2], \quad K = [0 \quad C_c] \end{aligned} \quad (17)$$

The augmented system can be written as

$$\begin{aligned} \dot{\eta}(t) &= A_{cl} \eta(t) + A_d \eta(t - \tau(t)) - (B_{cl} + \mathbb{R} E_c) \psi(K \eta(t)) \\ &\quad + B_{cl,\omega} \omega(t) \\ z(t) &= C_{cl,z} \eta(t) + D_{cl,z} \psi(K \eta(t)) \end{aligned} \quad (18)$$

where $\psi(K \eta(t)) = y_c(t) - \text{sat}(y_c(t))$ is a dead-zone non-linearity.

Lemma 1: Consider a dead-zone sector condition non-linearity $\psi(K \eta(t))$. If $\eta(t) \in \mathbb{S}$, then $\psi(K \eta(t))$ is always satisfies the following inequality [18]:

$$\psi(K \eta(t))' Q (\psi(K \eta(t)) + F \eta(t)) \leq 0, \quad (19)$$

where

$$\mathbb{S} = \eta \in \mathfrak{R}^{n_p + n_c}, \quad y_{c_{\min}} \leq (K - F)\eta \leq y_{c_{\max}} \quad (20)$$

is a polyhedral set with a matrix $F \in \mathfrak{R}^{m \times (n_p + n_c)}$, and $Q \in \mathfrak{R}^{m \times m}$ is any positive definite diagonal matrix.

3 Anti-windup synthesis with time-delay

The designed damping controller (4) using Remark 1, guarantees the asymptomatic stability of the closed-loop system in the absence of actuator saturation and time-delays. In this section, we propose an AWC design using delay dependent Lyapunov-Krasovskii functional to compensate the effect of actuator saturation and time-delays simultaneously. The sufficient conditions are formulated in the form of LMIs are given in the following theorem.

Theorem 1: For a given scalars $h > 0$, $d > 0$, and $\alpha > 0$, the closed-loop system (18) with AWC gain $E_c = \nu J^{-1}$ is asymptotically stable and possess H_∞ performance γ for actuator saturation and any time-varying delay $\tau(t)$ satisfying (11) and (12), respectively, if there exist a positive definite symmetric matrices \bar{X} , \bar{Y} , and \bar{Z} , a positive diagonal matrix J and any matrices P , \bar{G} , \bar{H} , W , ν and a positive scalar γ satisfying the following LMIs:

$$\begin{bmatrix} \Omega_{11} & \Omega_{12} & \Omega_{13} & \Omega_{14} & B_{cl,\omega} & h\bar{G} & PC'_{cl,z} \\ * & \Omega_{22} & \alpha A_d P' & \Omega_{24} & \alpha B_{cl,\omega} & 0 & 0 \\ * & * & \Omega_{33} & 0 & 0 & h\bar{H} & 0 \\ * & * & * & -2J & 0 & 0 & -JD'_{cl,z} \\ * & * & * & * & -I & 0 & 0 \\ * & * & * & * & * & -h\bar{Z} & 0 \\ * & * & * & * & * & * & -\gamma I \end{bmatrix} < 0, \quad (21)$$

$$\begin{bmatrix} \bar{X} & PK'_{(i)} - W'_{(i)} \\ * & \mu u_{0i}^2 \end{bmatrix} \geq 0, \quad i = 1, \dots, m. \quad (22)$$

where

$$\begin{aligned} \Omega_{11} &= A_{cl} P' + P A'_{cl} + \bar{Y} + \bar{G} + \bar{G}', \quad \Omega_{12} = \bar{X} - P' + \alpha P A' \\ \Omega_{13} &= -\bar{G} + \bar{H}' + A_d P', \quad \Omega_{14} = - (B_{cl} J + \mathbb{R} \nu) + W' \\ \Omega_{22} &= -\alpha P' - \alpha P + h\bar{Z}, \quad \Omega_{24} = -\alpha (B_{cl} J + \mathbb{R} \nu) \\ \Omega_{33} &= -\bar{H} - \bar{H}' - (1-d)\bar{Y}. \end{aligned}$$

and

$$u_{0i} = \min \{y_{c_{\max(i)}}, y_{c_{\min(i)}}\}.$$

Proof: Consider the following Lyapunov candidate function:

$$V(t) = \eta'(t)X\eta(t) + \int_{t-\tau(t)}^t \eta'(s)Y\eta(s) ds + \int_{-h}^0 \int_{t+\theta}^t \dot{\eta}'(s)Z\dot{\eta}(s) ds d\theta \quad (23)$$

where X , Y and Z are positive definite symmetric matrices which are to be determined.

The time derivative of $V(t)$ along the trajectories of the closed-loop system (18) is given by

$$\begin{aligned} \dot{V}(t) &= \dot{\eta}'(t)X\eta(t) + \eta'(t)X\dot{\eta}(t) \\ &+ \eta'(t)Y\eta(t) - (1-d)\eta'(t-\tau(t))Y\eta(t-\tau(t)) \\ &+ h\dot{\eta}'(t)Z\dot{\eta}(t) - \int_{t-h}^t \dot{\eta}'(s)Z\dot{\eta}(s) ds \end{aligned} \quad (24)$$

From (11), it is clear that the following is true:

$$- \int_{t-h}^t \dot{\eta}'(s)Z\dot{\eta}(s) ds \leq - \int_{t-\tau(t)}^t \dot{\eta}'(s)Z\dot{\eta}(s) ds \quad (25)$$

By using (25), we can rewrite $\dot{V}(\hat{x}_c(t))$ as follows

$$\begin{aligned} \dot{V}(t) &\leq \dot{\eta}'(t)X\eta(t) + \eta'(t)X\dot{\eta}(t) \\ &+ \eta'(t)Y\eta(t) - (1-d)\eta'(t-\tau(t))Y\eta(t-\tau(t)) \\ &+ h\dot{\eta}'(t)Z\dot{\eta}(t) - \int_{t-\tau(t)}^t \dot{\eta}'(s)Z\dot{\eta}(s) ds \end{aligned} \quad (26)$$

By using Lemma 2.1 from [31], we can expand $\int_{t-\tau(t)}^t \dot{\eta}'(s)Z\dot{\eta}(s) ds$ as follows:

$$\begin{aligned} - \int_{t-\tau(t)}^t \dot{\eta}'(s)Z\dot{\eta}(s) ds &\leq 2[\eta'(t) \quad \eta'(t-\tau(t))] \begin{bmatrix} G & -G \\ H & -H \end{bmatrix} \\ &\times \begin{bmatrix} \eta(t) \\ \eta(t-\tau(t)) \end{bmatrix} + h[\eta'(t) \quad \eta'(t-\tau(t))] \\ &\times \begin{bmatrix} G \\ H \end{bmatrix} Z^{-1} [G' \quad H'] \begin{bmatrix} \eta(t) \\ \eta(t-\tau(t)) \end{bmatrix} \end{aligned} \quad (27)$$

By using sector condition from Lemma 1, the time derivative of $V(t)$ is extended to

$$\dot{V}(t) \leq \dot{V}(t) - 2\psi(\mathbf{K}\eta(t))' \mathbf{Q}(\psi(\mathbf{K}\eta(t)) - \mathbf{F}\eta(t)) \quad (28)$$

By using free-weighting matrix method [32], the following relation holds for the appropriately sized matrices $\mathbf{P}_1, \mathbf{P}_2$:

$$0 = 2[\eta'(t)\mathbf{P}_1 + \dot{\eta}'(t)\mathbf{P}_2] \times [-\dot{\eta}(t) + A_{cl}\eta(t) + A_d\eta(t-\tau(t)) - (\mathbf{B}_{cl} + \mathbb{R}E_c)\psi(\mathbf{K}\eta(t)) + \mathbf{B}_{cl,\omega}\omega(t)] \quad (29)$$

Then, adding the terms on the right of (27) and (29) into (28), we have

$$\begin{aligned} \dot{V}(t) &\leq \dot{\eta}'(t)X\eta(t) + \eta'(t)X\dot{\eta}(t) \\ &+ \eta'(t)Y\eta(t) - (1-d)\eta'(t-\tau(t))Y\eta(t-\tau(t)) \\ &+ h\dot{\eta}'(t)Z\dot{\eta}(t) + 2[\eta'(t) \quad \eta'(t-\tau(t))] \begin{bmatrix} G & -G \\ H & -H \end{bmatrix} \\ &\times \begin{bmatrix} \eta(t) \\ \eta(t-\tau(t)) \end{bmatrix} + h[\eta'(t) \quad \eta'(t-\tau(t))] \begin{bmatrix} G \\ H \end{bmatrix} Z^{-1} [G' \quad H'] \\ &\times \begin{bmatrix} \eta(t) \\ \eta(t-\tau(t)) \end{bmatrix} + 2[\eta'(t)\mathbf{P}_1 + \dot{\eta}'(t)\mathbf{P}_2] \times [-\dot{\eta}(t) + A_{cl}\eta(t) \\ &+ A_d\eta(t-\tau(t)) - (\mathbf{B}_{cl} + \mathbb{R}E_c)\psi(\mathbf{K}\eta(t)) + \mathbf{B}_{cl,\omega}\omega(t)] \\ &- 2\psi(\mathbf{K}\eta(t))' \mathbf{Q}(\psi(\mathbf{K}\eta(t)) - \mathbf{F}\eta(t)) \end{aligned} \quad (30)$$

Define an auxiliary function for the H_∞ performance of the system (18)

$$M(t) = \dot{V}(t) - \omega'(t)\omega(t) + \frac{1}{\gamma}z'(t)z(t) \quad (31)$$

and it can be simplified as follows:

$$\begin{aligned} M(t) &\leq \xi'(t)\Lambda\xi(t) + h[\eta'(t) \quad \eta'(t-\tau(t))] \begin{bmatrix} G \\ H \end{bmatrix} Z^{-1} \\ &\times [G' \quad H'] \begin{bmatrix} \eta(t) \\ \eta(t-\tau(t)) \end{bmatrix} + [\eta'(t) \quad \psi(\mathbf{K}\eta(t))]' \\ &\times \begin{bmatrix} C'_{cl,z} \\ -D'_{cl,z} \end{bmatrix} \frac{1}{\gamma} [C_{cl,z} \quad -D_{cl,z}] \begin{bmatrix} \eta(t) \\ \psi(\mathbf{K}\eta(t)) \end{bmatrix} \end{aligned} \quad (32)$$

where

$$\Lambda = \begin{bmatrix} \Lambda_{11} & \Lambda_{12} & \Lambda_{13} & \Lambda_{14} & \mathbf{P}_1\mathbf{B}_{cl,\omega} \\ * & \Lambda_{22} & \mathbf{P}_2A_d & -\mathbf{P}_2(\mathbf{B}_{cl} + \mathbb{R}E_c) & \mathbf{P}_2\mathbf{B}_{cl,\omega} \\ * & * & \Lambda_{33} & 0 & 0 \\ * & * & * & -2\mathbf{Q} & 0 \\ * & * & * & * & -I \end{bmatrix}$$

$$\Lambda_{11} = \mathbf{P}_1A_{cl} + A'_{cl}\mathbf{P}'_1 + \mathbf{Y} + \mathbf{G} + \mathbf{G}', \quad \Lambda_{12} = \mathbf{X} - \mathbf{P}_1 + A'_{cl}\mathbf{P}'_1$$

$$\Lambda_{13} = -\mathbf{G} + \mathbf{H}' + \mathbf{P}_1A_d, \quad \Lambda_{14} = -\mathbf{P}_1(\mathbf{B}_{cl} + \mathbb{R}E_c) + \mathbf{F}'\mathbf{Q}$$

$$\Lambda_{22} = -\mathbf{P}_2 - \mathbf{P}'_2 + h\mathbf{Z}, \quad \Lambda_{33} = -\mathbf{H} - \mathbf{H}' - (1-d)\mathbf{Y}$$

with

$$\xi'(t) = [\eta'(t) \quad \dot{\eta}'(t) \quad \eta'(t-\tau(t)) \quad \psi(\mathbf{K}\eta(t))' \quad \omega'(t)]$$

Using Schur complement [33], the inequality (32) is equal to

$$M(t) \leq \xi'(t)\Psi\xi(t) \quad (33)$$

where

$$\Psi = \begin{bmatrix} \Psi_{11} & \Psi_{12} & \Psi_{13} & \Psi_{14} & \mathbf{P}_1\mathbf{B}_{cl,\omega} & h\mathbf{G} & C'_{cl,z} \\ * & \Psi_{22} & \mathbf{P}_2A_d & \Psi_{24} & \mathbf{P}_2\mathbf{B}_{cl,\omega} & 0 & 0 \\ * & * & \Psi_{33} & 0 & 0 & h\mathbf{H} & 0 \\ * & * & * & -2\mathbf{Q} & 0 & 0 & -D'_{cl,z} \\ * & * & * & * & -I & 0 & 0 \\ * & * & * & * & * & -h\mathbf{Z} & 0 \\ * & * & * & * & * & * & -\gamma\mathbf{I} \end{bmatrix}$$

$$\Psi_{11} = \mathbf{P}_1A_{cl} + A'_{cl}\mathbf{P}'_1 + \mathbf{Y} + \mathbf{G} + \mathbf{G}', \quad \Psi_{12} = \mathbf{X} - \mathbf{P}_1 + A'_{cl}\mathbf{P}'_1$$

$$\Psi_{13} = -\mathbf{G} + \mathbf{H}' + \mathbf{P}_1A_d, \quad \Psi_{14} = -\mathbf{P}_1(\mathbf{B}_{cl} + \mathbb{R}E_c) + \mathbf{F}'\mathbf{Q}$$

$$\Psi_{22} = -\mathbf{P}_2 - \mathbf{P}'_2 + h\mathbf{Z}, \quad \Psi_{24} = -\mathbf{P}_2(\mathbf{B}_{cl} + \mathbb{R}E_c)$$

$$\Psi_{33} = -\mathbf{H} - \mathbf{H}' - (1-d)\mathbf{Y}$$

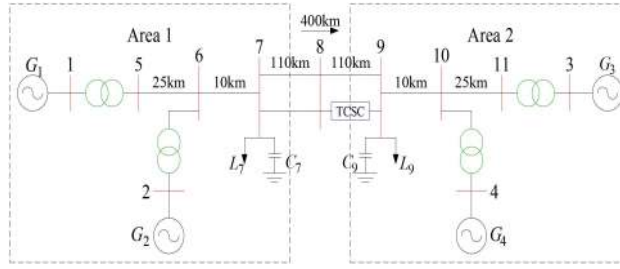


Fig. 2 Line diagram of two-area four-machine system

Table 1 Inter- and local-area modes of two-area four-machine system

Modes	Inter		Local 1		Local 2	
	ζ	f , Hz	ζ	f , Hz	ζ	f , Hz
WC	0.0717	0.6534	0.1752	1.2186	0.1684	1.2686
HwoDS	0.1567	0.6371	0.1751	1.2194	0.1674	1.2700
PC	0.3283	0.6450	0.1721	1.2191	0.1668	1.2686

WC – without controller, HwoDS – H_∞ controller without delays and saturation, PC – proposed controller.

From (33), if $\Psi < 0$, then the auxiliary function $M(t)$ is negative definite, which ensures that the closed-loop system is asymptotically stable.

To solve an AWC gain E_c , introduce some change of variables as

$$\begin{aligned} P &= P_1^{-1}, \quad \bar{X} = PXP', \quad \bar{Y} = PYP', \quad \bar{Z} = PZP' \\ \bar{G} &= PGP', \quad \bar{H} = PHP', \quad J = Q^{-1}, \\ W &= FP', \quad \nu = E_c Q^{-1} \end{aligned}$$

Considering $P_2 = \alpha P_1$, where α is a scalar tuning parameter and pre- and post-multiply the inequality $\Psi < 0$ by Π and Π' , respectively, with $\Pi = \text{diag}\{P_1^{-1}, P_1^{-1}, P_1^{-1}, Q^{-1}, I, P_1^{-1}, I\}$, i.e.

$$\Pi \Psi \Pi' < 0 \quad (34)$$

From inequality (34), we obtain the inequality (21).

To include actuator saturation in the controller design, we consider a sector constraint as follows:

$$(K_i - F_i)'(K_i - F_i) \leq u_{0i}^2 X, \quad i = 1, \dots, m. \quad (35)$$

By using Schur complement, we can rewrite (35) as

$$\begin{bmatrix} X & K_i' - F_i' \\ & u_{0i}^2 \end{bmatrix} \geq 0, \quad i = 1, \dots, m. \quad (36)$$

Pre- and post-multiply inequality (36) by

$$\begin{bmatrix} P & 0 \\ 0 & I \end{bmatrix} \quad \text{and} \quad \begin{bmatrix} P' & 0 \\ 0 & I \end{bmatrix},$$

respectively and we get the inequality (22), which concludes proof of the theorem. \square

4 Case study: a two-area four-machine power system

4.1 System description

The benchmark model of the two-area four-machine power system is considered to validate the efficiency of the proposed controller as shown in Fig. 2, which is widely used for studying the low-frequency oscillations. The system consists of two areas and each area consists of two generators and five buses. These two areas are weakly connected by tie-line buses, so there are total of 11 buses and 4 generators in the whole system. The synchronous generators $G_i (i = 1, 2, 3, 4)$ are represented by a sixth-order sub-transient

model with state variables $\delta, \omega, E_d', E_q', \psi_{1d}, \psi_{2q}$, which are equipped with a simple, fast acting first-order IEEE-ST1A type static excitation system. To damp out the local area oscillations G_1 and G_3 are equipped with a third-order PSS. The line data, bus data and the parameters of generators, PSS, and exciters are given in [34].

In normal operating condition, active power flows from Area 1 to Area 2 is ~ 400 MW. To improve the power transfer capability and enhance the damping of inter-area oscillations, a series FACTS device, i.e. a TCSC is connected in series with the transmission line #8-#9. The initial percentage compensation $\%k_c$ of TCSC is considered 10% with 50 and 1% as their upper and lower limits in the presence of supplementary damping controller.

4.2 Modal analysis and model-order reduction

From eigenvalue analysis, three electromechanical modes of oscillations are presented in the four-machine two-area system as shown in Table 1. Out of these three modes, two are local modes and one is inter-area mode. Modal controllability and observability [34] have been used to select a suitable controller placement and feedback signals for damping controller design. A TCSC connected at line #8-#9 is taken the controller location and active power deviation of line #10-#9 (ΔP_{10-9}) is taken as a feedback signal, these having higher controllability and observability corresponding to the critical oscillatory mode.

By considering the control signal of TCSC ($\%k_c$) as the input and ΔP_{10-9} as a feedback output signal, the power system model is linearised at the equilibrium point. The size of the linearised model is 34th order resulting in complexity in the controller design. To make the controller design convenient and feasible, model order reduction is required. By using *Schur* balanced model reduction method [30], the original system is reduced to 8th order. The reduced-order model will remain the information about the poorly damped oscillatory modes. The frequency responses of both full and reduced-order model are shown in Fig. 3. From the frequency response, 8th-order reduced model is used for the design of the proposed controller.

4.3 Results and discussion

The reduced 8th-order linearised open-loop power system model (3) is used to design the proposed damping controller.

First of all, the SDC of TCSC device is designed for the reduced model (3) by using H_∞ output feedback control with pole placement approach presented in Remark 1, without considering the effects of actuator saturation and time-delays. For H_∞ output feedback control, the frequency dependent weighting matrices are chosen as follows:

$$W_1 = \frac{30}{s+30}, \quad W_2 = \frac{10s}{s+100}. \quad (37)$$

To ensure the minimum damping ratio of 0.15 for the closed-loop system, a conic sector region \mathfrak{D} with an inner angle $2\cos^{-1}0.15$ with the apex at the origin is selected for the pole-placement region. The order of the designed controller from Remark 1 is equal to the order of reduced model plus order of the weights. The 10th order of the controller is again reduced to 8th order by using *Schur* balanced model reduction method.

Simulation studies are carried out on a non-linear power system model in MATLAB/Simulink to evaluate the effectiveness of the H_∞ output feedback controller designed without considering time-delays and actuator saturation. A three-phase to ground fault is considered as a disturbance on the power system which takes place in a transmission line #8-#9 at 1 s with duration of 100 ms at 400 MW tie-line active power flow as an attempt to excite the inter-area mode. The response of the speed deviation of $G_1 - G_3$ and percentage compensation of TCSC ($\%k_c$) is depicted in Figs. 4 and 5 to show the effect of actuator saturation and time-delays on the damping of inter-area oscillations and therefore effect on the closed-loop performance when the controller is designed without considering time-delays and actuator saturation.

4.3.1 Effect of actuator saturation: The effect of actuator saturation on the closed-loop performance (regarding speed deviation of $G_1 - G_3$ and percentage compensation of TCSC ($\%k_c$)) is depicted in Fig. 4. From Fig. 4, we can observe that when the actuator output is limited by minimum and maximum values there will be saturation occurs in the response of $\%k_c$ of TCSC and due

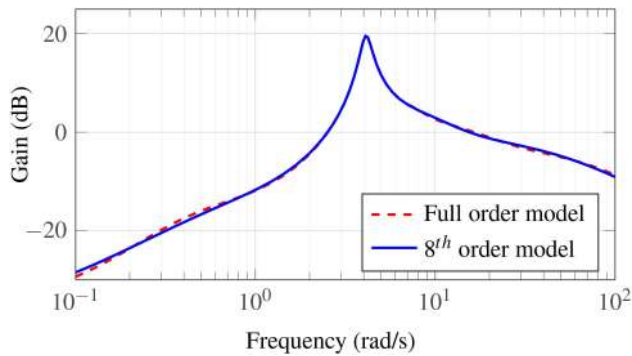


Fig. 3 Frequency response of the full-order versus the reduced-order system

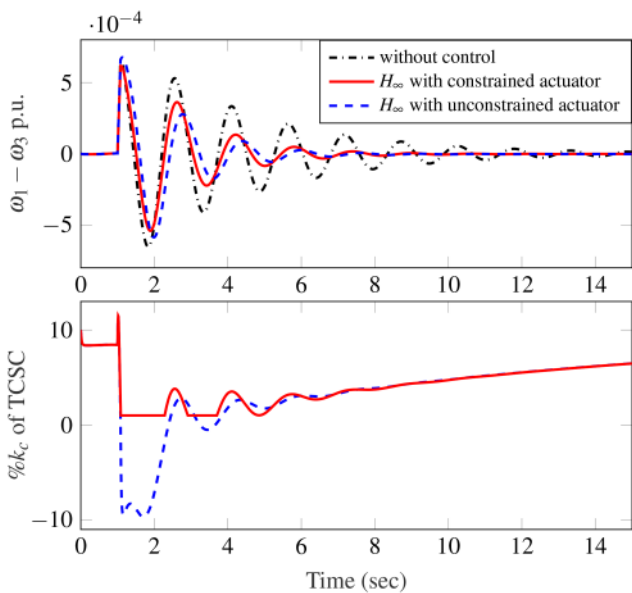


Fig. 4 Effect of actuator saturation on the performance of the case study

to saturation the damping of the oscillation mode is deteriorated as indicated in the transient response of the speed deviation of $G_1 - G_3$. For the comparison purpose, the transient response of the speed deviation of $G_1 - G_3$ and percentage compensation of TCSC ($\%k_c$) are also shown in Fig. 4 when the actuator output is not limited by minimum and maximum values in the simulation. The comparison of responses of the speed deviation with and without constrained actuator confirms that the damping predicted in the controller design is not achieved due to the actuator saturation presence. The limits of the actuator are unavoidable due to the physical and security limitation of the actuator. So to mitigate the effect of actuator saturation, it is necessary to consider the actuator saturation constraints in the design procedure of the controller. In this work, an add-on AWC is designed for the H_∞ output feedback controller to minimise the effect caused by the actuator saturation.

4.3.2 Effect of time-delay: The effect of time-delay on the closed-loop performance is depicted in Fig. 5 when H_∞ output feedback controller designed without considering time-delays and actuator saturation. From Fig. 5, we can observe that the H_∞ output feedback controller exhibits satisfactory results to damp the inter-area oscillations when there is no delay (i.e. $h = 0$ ms) in the feedback signal. But when the time delay occurs and increases, the damping of the inter-area mode is deteriorated and the controller is incapable of providing satisfactory performance of the closed-loop system. When the time-delay increase, the control signal is saturating more and that is degrading the performance of the closed-loop system. The responses in Fig. 5 prove that the time-delays in the feedback loop will degrade the performance and even lead to instability of the closed-loop power system. To compensate the effect of time-delays, it is necessary to consider the time-delays in the controller design.

To overcome actuator saturation and time-delay problems simultaneously, we propose a delay-dependent AWC by using Lyapunov-Krasovskii functional.

To compute an AWC gain E_c , the proposed problem is converted into a convex optimisation problem, which ensures the stability of the closed-loop system (18) for time-delays and saturation satisfying (11) and (12), respectively. To minimise the upper bound for L_2 a gain of $\omega(t)$ on $z(t)$, consider the following convex optimisation problem

$$\begin{aligned} & \min \gamma \\ & \text{s. t. LMI's (21) and (22)}. \end{aligned} \quad (38)$$

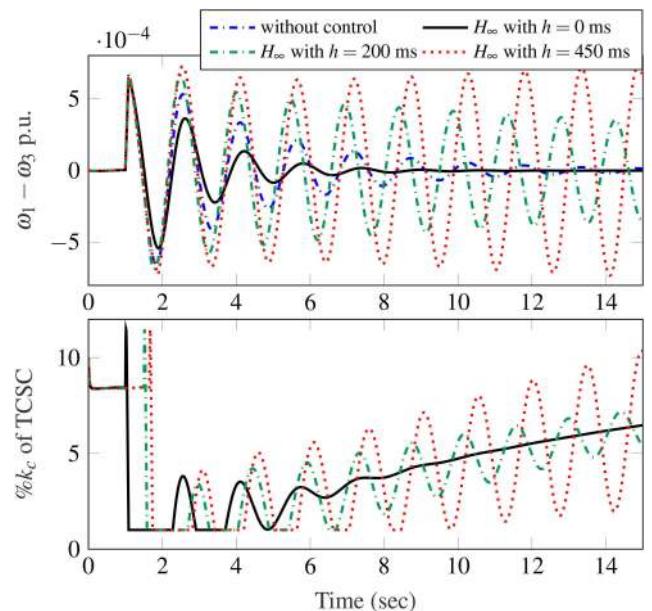


Fig. 5 Effect of time delays on the performance of the case study

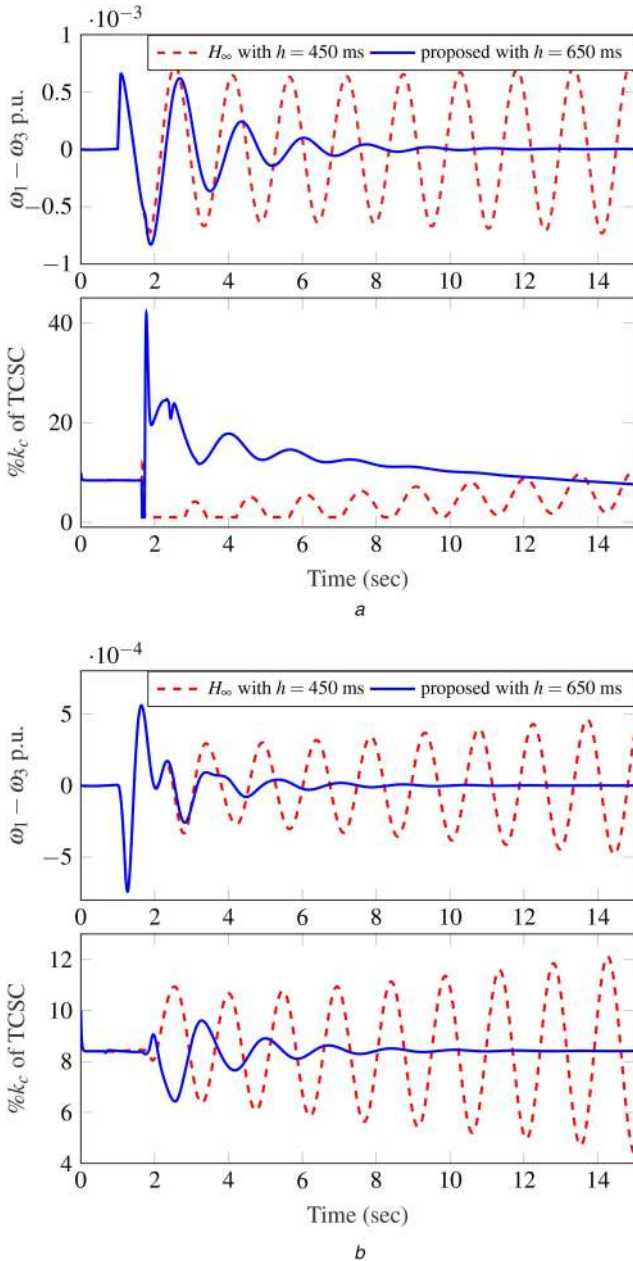


Fig. 6 MATLAB simulation responses of case study for scenarios 1 and 2 with proposed controller compared with H_∞ controller
(a) Dynamic response of case study for scenario 1, (b) Dynamic response of case study for scenario 2

The optimisation problem (38) is solved for the closed-loop system (18) by using LMI toolbox in MATLAB with $d = 0.1$, $\alpha = 0.7$, $\gamma_{c_{\max}} = 0.5$, $\gamma_{c_{\min}} = 0.01$, and for delay margin $h = 650$ ms, we obtain $\gamma = 55.09$ and an AWC gain

$$E_c = \begin{bmatrix} 16.4929 & 2.1922 & -9.8625 & 0.5598 \\ 17.9987 & 0.7247 & 2.8049 & 0.7848 \end{bmatrix}^T \quad (39)$$

The efficiency of the proposed damping controller is verified by the following two scenarios.

Scenario 1: A three-phase to ground fault takes place on a transmission line #8-#9 at 1 s with a duration of 100 ms.

Scenario 2: The generator G_1 terminal voltage increases +5% step at 1 s.

The responses of the rotor speed deviation of the generator 1 and generator 3 ($\omega_1 - \omega_3$) and percentage compensation of TCSC ($\%k_c$) of a case study with the proposed controller, compared with

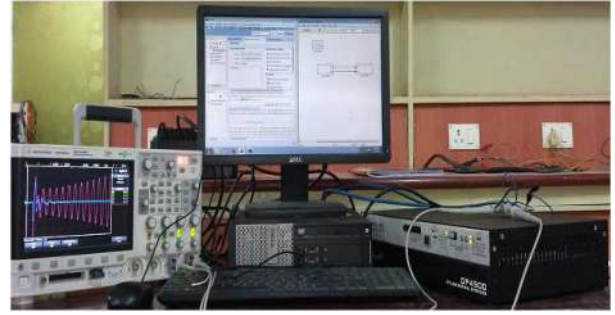


Fig. 7 Experimental set-up of OPAL-RT OP4500 simulator

H_∞ output feedback control with pole placement are shown in Fig. 6 for scenarios 1 and 2. From dynamic responses shown in Fig. 6, it can be observed that the H_∞ output feedback controller designed without considering time-varying delays and actuator saturation provides less damping to inter-area oscillations when the time-delay $h = 450$ ms occurs in the feedback loop and the control signal is saturated by reaches its maximum value. However, the proposed controller successfully damps out the inter-area low-frequency oscillation even when the time-delay $h = 650$ ms occurs by providing sufficient damping under different operating conditions. From the response of TCSC output, it is observed that the H_∞ output feedback controller exhibits actuator saturation at different operating conditions, but the proposed controller reduces the saturation region and improves the dynamic performance of the closed-loop system.

5 Real-time simulation (RTS) results

RTS is an integral part of research and development of power systems and other engineering fields [35]. RTSs are performed in OPAL-RT OP4500 real-time digital simulator using INTEL multi-core processors with Xilinx Kintex 7 FPGA MMPK7 board. OPAL-RT provides a distributed real-time platform and it allows to model and simulates the power system in MATLAB/Simulink with high accuracy, low cost and small time-steps to precisely emulate the actual power system. The efficiency of the proposed controller is demonstrated in real-time fewer than two different scenarios of the case study. The experimental set-up of OPAL-RT OP4500 simulator is shown in Fig. 7. The detailed non-linear power system with damping controller is modelled in MATLAB/Simulink and further editing is performed to make it to compatible with Opal-RT by using its RT-LAB library. Then, the model is split into two subsystems, e.g. master subsystem, where plant and controller are kept and console subsystem, where outputs are displayed. The total split model is loaded into the Opal-RT server to convert it to C code. By setting solver time-step as fixed time-step mode with time-step of 0.8 ms, the program is executed. The results obtained from the simulator are shown in Fig. 8. From the RTSs for both operating conditions, it can be observed that the proposed damping controller guarantees the performance and stability of closed-loop wide-area power system with time-delays and actuator saturation in real-time.

6 Conclusions

The problem of time-delays with actuator saturation and its influence on the performance and stability of a closed-loop system has been studied for years, but the control approaches for power systems with actuator saturation have been rarely investigated. The power system actuators are subjected to the limited magnitude and the time-delays are inevitable in the feedback loop. If these constraints are not considered in the design procedure of the controller, the damping performance of the controller maybe degraded or even lead to the instability of the closed-loop power system. The main contribution of this work is to design a delay-dependent AWC for the power system with time-delays and actuator saturation to enhance the damping of inter-area oscillations. Sufficient conditions required for the asymptotic stability of the closed-loop power system are derived by using

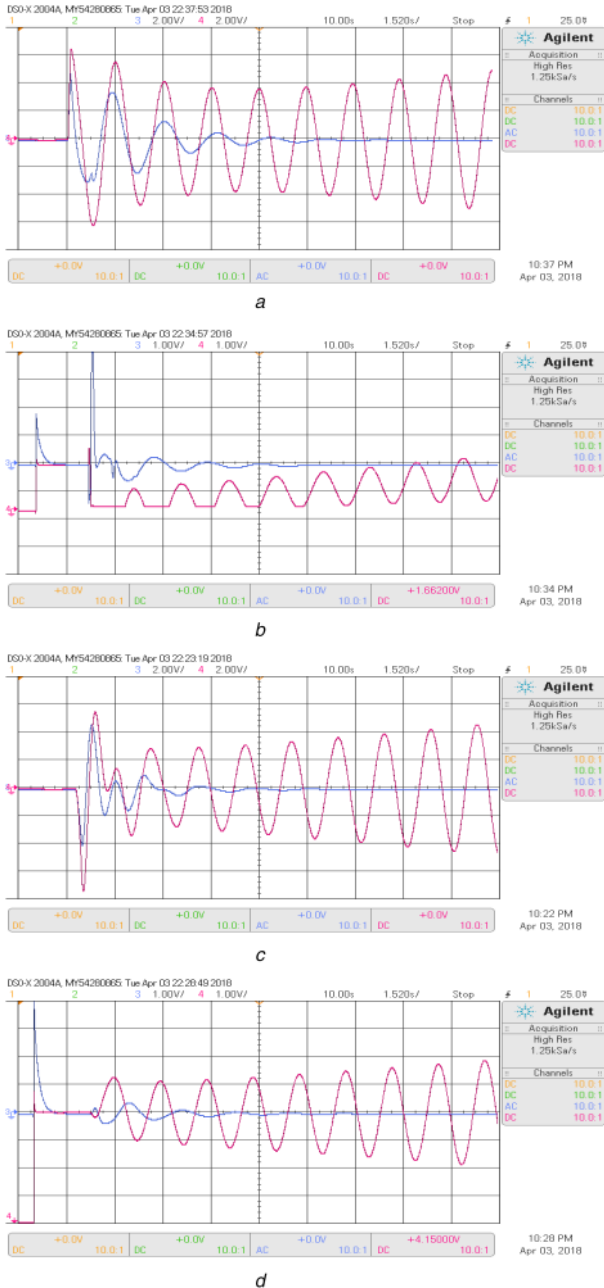


Fig. 8 RTS responses of case study for scenarios 1 and 2 with proposed controller ($h = 650$ ms) compared with H_∞ controller ($h = 450$ ms) (a) Speed deviation response of $\omega_1 - \omega_3$ of case study for scenario 1, (b) TSCS output response of case study for scenario 1, (c) Speed deviation response of $\omega_1 - \omega_3$ of case study for scenario 2, (d) TSCS output response of case study for scenario 2

Lyapunov–Krasovskii functional and generalised sector condition. These conditions are then formulated as an LMI convex optimisation, allowing the proposed controller to minimise the L_2 -gain of the disturbance $\omega(t)$ to the system regulated output $z(t)$.

The efficiency of the proposed controller is validated by implementing the case study namely a two-area four-machine power system in both MATLAB/Simulink and OPAL-RT real-time simulator. From results obtained from both MATLAB/Simulink and real-time simulator, it clearly shows that the H_∞ output feedback controller not provides sufficient damping to the inter-area oscillations when the time-delay occur in the feedback and the control signals subjected to actuator saturation. However, the proposed controller exhibits excellent performance in the presence of time-delays and actuator saturation and provides sufficient damping to the inter-area oscillations as compared to H_∞ output feedback controller.

7 References

- [1] Rogers, G.: ‘Power system oscillations’ (Springer Science & Business Media, New York, 2012)
- [2] Wu, H., Tsakalis, K.S., Heydt, G.T.: ‘Evaluation of time delay effects to wide-area power system stabilizer design’, *IEEE Trans. Power Syst.*, 2004, **19**, (4), pp. 1935–1941
- [3] Chompoobutgool, Y., Vanfretti, L., Ghandhari, M.: ‘Survey on power system stabilizers control and their prospective applications for power system damping using synchrophasor-based wide-area systems’, *Int. Trans. Electr. Energy Syst.*, 2011, **21**, (8), pp. 2098–2111
- [4] Shakarami, M., Davoudkhani, I.F.: ‘Wide-area power system stabilizer design based on grey wolf optimization algorithm considering the time delay’, *Electr. Power Syst. Res.*, 2016, **133**, pp. 149–159
- [5] Li, Y., Rehtanz, C., Ruberg, S., et al.: ‘Wide-area robust coordination approach of HVDC and FACTS controllers for damping multiple interarea oscillations’, *IEEE Trans. Power Deliv.*, 2012, **27**, (3), pp. 1096–1105
- [6] Yao, W., Jiang, L., Wen, J., et al.: ‘Wide-area damping controller of FACTS devices for inter-area oscillations considering communication time delays’, *IEEE Trans. Power Syst.*, 2014, **29**, (1), pp. 318–329
- [7] Deng, J., Li, C., Zhang, X.P.: ‘Coordinated design of multiple robust FACTS damping controllers: a BMI-based sequential approach with multi-model systems’, *IEEE Trans. Power Syst.*, 2015, **30**, (6), pp. 3150–3159
- [8] Kamwa, I., Grondin, R., Hébert, Y.: ‘Wide-area measurement based stabilizing control of large power systems—a decentralized/hierarchical approach’, *IEEE Trans. Power Syst.*, 2001, **16**, (1), pp. 136–153
- [9] Zhang, W., Branicky, M.S., Phillips, S.M.: ‘Stability of networked control systems’, *IEEE Control Syst.*, 2001, **21**, (1), pp. 84–99
- [10] Li, Y., Zhou, Y., Liu, F., et al.: ‘Design and implementation of delay-dependent wide-area damping control for stability enhancement of power systems’, *IEEE Trans. Smart Grid*, 2017, **8**, (4), pp. 1831–1842
- [11] Singh, A.K., Singh, R., Pal, B.C.: ‘Stability analysis of networked control in smart grids’, *IEEE Trans. Smart Grid*, 2015, **6**, (1), pp. 381–390
- [12] Wang, S., Meng, X., Chen, T.: ‘Wide-area control of power systems through delayed network communication’, *IEEE Trans. Control Syst. Technol.*, 2012, **20**, (2), pp. 495–503
- [13] Molina-Cabrera, A., Ros, M.A., Besanger, Y., et al.: ‘A latencies tolerant model predictive control approach to damp inter-area oscillations in delayed power systems’, *Int. J. Electr. Power Energy Syst.*, 2018, **98**, pp. 199–208
- [14] Fan, R., Huang, R., Sun, L.: ‘Nonlinear model predictive control of HVDC for inter-area oscillation damping’, *Electr. Power Syst. Res.*, 2018, **165**, pp. 27–34
- [15] Azad, S.P., Iravani, R., Tate, J.E.: ‘Damping inter-area oscillations based on a model predictive control (MPC) HVDC supplementary controller’, *IEEE Trans. Power Syst.*, 2013, **28**, (3), pp. 3174–3183
- [16] Jain, A., Biyik, E., Chakraborty, A.: ‘A model predictive control design for selective modal damping in power systems’. IEEE American Control Conf. (ACC), Chicago, July 2015, pp. 4314–4319
- [17] Hu, T., Lin, Z.: ‘Control systems with actuator saturation: analysis and design’ (Springer Science & Business Media, New York, 2001)
- [18] Tarbouriech, S., Garcia, G., da Silva, J.M.G.Jr., et al.: ‘Stability and stabilization of linear systems with saturating actuators’ (Springer Science & Business Media, London, 2011)
- [19] Dang, Q.V., Vermeiren, L., Dequidt, A., et al.: ‘Robust stabilizing controller design for Takagi–Sugeno fuzzy descriptor systems under state constraints and actuator saturation’, *Fuzzy Sets Syst.*, 2017, **PP**, (99), pp. 1–1
- [20] Hu, T., Teel, A.R., Zaccarian, L.: ‘Stability and performance for saturated systems via quadratic and nonquadratic Lyapunov functions’, *IEEE Trans. Autom. Control*, 2006, **51**, (11), pp. 1770–1786
- [21] Lu, L., Lin, Z.: ‘Design of switched linear systems in the presence of actuator saturation’, *IEEE Trans. Autom. Control*, 2008, **53**, (6), pp. 1536–1542
- [22] Zhang, X.Q., Zhao, J.: ‘ L_2 -gain analysis and anti-windup design of discrete-time switched systems with actuator saturation’, *Int. J. Autom. Comput.*, 2012, **9**, (4), pp. 369–377
- [23] Nguyen, T., Giunto, R.: ‘Optimal design for control coordination of power system stabilisers and flexible alternating current transmission system devices with controller saturation limits’, *IET Gener. Transm. Distrib.*, 2010, **4**, (9), pp. 1028–1043
- [24] Xin, H., Gan, D., Qu, Z., et al.: ‘Impact of saturation nonlinearities/disturbances on the small-signal stability of power systems: an analytical approach’, *Electr. Power Syst. Res.*, 2008, **78**, (5), pp. 849–860
- [25] Fang, J., Yao, W., Chen, Z., et al.: ‘Design of anti-windup compensator for energy storage-based damping controller to enhance power system stability’, *IEEE Trans. Power Syst.*, 2014, **29**, (3), pp. 1175–1185
- [26] Soliman, H.M., Yousef, H.A.: ‘Saturated robust power system stabilizers’, *Int. J. Electr. Power Energy Syst.*, 2015, **73**, pp. 608–614
- [27] Raoufat, M.E., Tomsovic, K., Djouadi, S.M.: ‘Power system supplementary damping controllers in the presence of saturation’. IEEE Power and Energy Conf. (PECI), Illinois, 2017, pp. 1–6
- [28] Gahinet, P.: ‘ H_∞ design with pole placement constraints: an LMI approach’, *IEEE Trans. Autom. Control*, 1996, **45**, (3), pp. 358–367
- [29] Pal, B., Chaudhuri, B.: ‘Robust control in power system’ (Springer, New York, U.S.A., 2005)
- [30] Chiang, M.G., Safonov, R.Y.: ‘A Schur method for balanced model reduction’, *IEEE Trans. Autom. Control*, 1989, **AC-34**, pp. 729–733
- [31] El-Haoussi, F., Tissir, E.H., Tadeo, F., et al.: ‘Delay-dependent stabilisation of systems with time-delayed state and control: application to a quadruple-tank process’, *Int. J. Syst. Sci.*, 2011, **42**, (1), pp. 41–49
- [32] He, Y., Wu, M., She, J.H., et al.: ‘Parameter-dependent Lyapunov functional for stability of time-delay systems with polytopic-type uncertainties’, *IEEE Trans. Autom. Control*, 2004, **49**, (5), pp. 828–832

- [33] Boyd, S., El-Ghaoui, L., Feron, E., *et al.*: '*Linear matrix inequalities in system and control theory*' (SIAM, Philadelphia, 1994)
- [34] Kundur, P., Balu, N.J., Lauby, M.G.: '*Power system stability and control*' (McGraw-Hill, New York, 1994)
- [35] Jiang, Z., Konstantinou, G., Zhong, Z., *et al.*: 'Real-time digital simulation based laboratory test-bench development for research and education on solar PV systems'. IEEE Universities Power Engineering Conf. (AUPEC), Australasian, 2017, pp. 1–6